Analytical Methods

PAPER

View Article Online
View Journal | View Issue

Cite this: *Anal. Methods*, 2015, **7**, 5114

New calix[4]arene based highly selective fluorescent probe for Al^{3+} and I^-†

Shahabuddin Memon,*[a] Ashfaque Ali Bhatti,[a] Ümmühan Ocak[b] and Miraç Ocak[b]

Received 18th February 2015
Accepted 30th April 2015

DOI: 10.1039/c5ay00452g

www.rsc.org/methods

This approach highlights the synthesis of a 2-hydroxy naphthalene functionalized calix[4]arene based fluorophoric Schiff base, **C4SB**. The ion-binding property of the **C4SB** fluoroionophore is probed with a number of cations and anions and the recognition events were monitored by UV-visible and fluorescence spectral changes. **C4SB** based on a photoinduced electron transfer mechanism exhibits a selective "turn-on" response towards Al^{3+} and a "turn-off" response for I^- in the presence of other competing ions with certain observable spectral changes. The selective behavior of the probe is visualized in the presence of competing ions. The interference study reveals that Hg^{2+} causes some disturbance to the **C4SB** and Al^{3+} interaction. **C4SB** forms a (1 : 1) stoichiometric complex with both Al^{3+} and I^- and their binding constants are calculated as 2.49×10^5 and 9.24×10^3, respectively. Moreover, the complexes were characterized through FT-IR spectroscopy.

Introduction

After oxygen and silicon, aluminum is the third most prevalent element in the lithosphere and is also abundant in the rest of the earth's crust. It has a variety of applications in daily life.[1,2] It is therapeutically beneficial but superfluous ingestion produces negative impacts on human beings and aquatic ecosystems.[3,4] Its accumulation in human tissues and organs causes various dysfunction and toxicity issues:[5,6] it inhibits the function of iron and sulfur containing proteins; bone and joint diseases including defective mineralization and osteomalacia;[7] neuronal disorders leading to dialysis encephalopathy, dementia, myopathy, idiopathic Parkinson's disease, impairment of memory, Alzheimer's disease;[8,9] and it may even cause lung, breast and bladder cancer.[10] Aluminium is also associated with anemia as it can increase hemolysis, and decrease heme and globulin synthesis. It directly effects iron metabolism; retarding its absorption and transportation.[11] People are generally prone to aluminum toxicity from its widespread use in various food and pharmaceutical utensils. According to a World Health Organization report the average daily human intake of aluminum is approximately 3–10 mg per day. Tolerable weekly aluminum intake in the human body is estimated to be 7 mg kg^{-1} of body weight.[12,13]

Research has also been devoted to the selective sensing of anions because of their importance in biological, medicinal, catalytic, environmental and chemical science.[14] Among the anionic species to be recognized and detected, I^- has received progressively more attention as its elemental form is widely utilized in chemistry for the synthesis of drugs and dyes.[15] It is one of the biologically important anions and is a significant micronutrient which plays a key role in many biological pathways such as brain development, metabolism, neurological functions and thyroid gland activity.[16] It is an essential element in life and is part of some thyroid hormones which are necessary for metabolism and brain development.[17] The recommended daily intake of iodide is 150 μg per day. Deficiency results in severe delays in neurological development, cretinism and endemic goiter. Conversely, excessive ingestion can cause hyperthyroidism.[18]

Determination of anions is a more challenging task compared to the detection of metal ions, which are usually discriminated on the basis of charge and size, as anions have complex structures and a larger size.[19] In this regard, a number of traditional advanced analytical techniques like ion chromatography,[20] capillary electrophoresis,[21] atomic absorption spectroscopy,[22] gas chromatography-mass spectrometry (GC-MS),[23] inductively coupled plasma (ICP)-MS,[24] electrochemical methods,[25] inductively coupled plasma atomic emission spectrometry (ICP-AES) or inductively coupled plasma mass spectrometry (ICP-MS) are the most commonly employed analytical techniques[26] used for the determination of both iodide and aluminum. Among them the fluorescence spectroscopic method is widely used because of its rapidity, sensitivity, selectivity, simplicity and cost-effectiveness.[27] Consequently, efficient and selective fluorescent probes are valuable

[a]*National Center of Excellence in Analytical Chemistry, University of Sindh, Jamshoro 76080, Pakistan. E-mail: shahabuddinmemon@yahoo.com; Fax: +92 22 2771560; Tel: +92 22 2772065*

[b]*Department of Chemistry, Faculty of Sciences, Karadeniz Technical University, Trabzon 61080, Turkey*

† Electronic supplementary information (ESI) available. See DOI: 10.1039/c5ay00452g

implements for the detection of biologically and environmentally important ions. The development of probes possessing high selectivity for Al^{3+} and I^- over other commonly coexisting ions in various media is of particular importance for environmental protection and human health. A variety of fluorescent probes have recently been exploited for the determination of Al^{3+} and I^-. In literature there are a few examples relating to "turn-on" and "turn-off" fluorescent probes available for both ions.[28–39]

With the advance of supramolecular chemistry, one of the most fascinating approaches is the development of highly specific, facile, and cost-effective chromogenic/fluorescent sensors for ions in biological media such as enzymes, antibodies or genes and is fundamental to supramolecular chemistry.[40,41] In this regard, macrocyclic calixarenes remain an area of interest due to their unique applicability for biomimic functions[42] ionic and molecular recognition[43] along with potential in the fundamental and applied sciences and coordination chemistry.[44] For ionic or molecular recognition calix[4] arenes are the most extensively employed molecular scaffolds as fluorescent sensors.[45] The synthesis of selective fluorescent sensors is a fundamental target for scientists. So far, there are some successful achievements in the development of calix[4] arene based fluorescent probes for Al^{3+} (ref. 46) and I^-.[47–49]

Herein, we designed and synthesized a new calix[4]arene based Schiff based fluorescent probe (**C4SB**), which displays highly selective and sensitive fluorescence "turn-on" recognition to Al^{3+} and turn-off fluorescence emission behavior for I^-.

Experimental

Chemicals

All reagents and solvents used were of standard analytical grade purchased from Alfa Aesar (Germany), Merck (Darmstadt, Germany) and were used without further purification. All metal nitrate salts and sodium salts of anions were purchased from Sigma and Aldrich. All aqueous solutions were prepared with deionized water that had been passed through a millipore milli Q Plus water purification system.

Instrumentation

Melting points were determined on a Gallenkamp (UK) apparatus in a sealed capillary tube. Elemental analyses (CHNS) were performed using a Flash EA 1112 elemental analyzer. ^1H and ^{13}C NMR spectra were recorded with an Agilent 400 MHz spectrometer in DMSO using tetramethylsilane (TMS) as an internal standard at room temperature. Thermo Nicollet AVATAR 5700 FT-IR spectrometer was used for recording IR spectra within a spectral range from 4000 to 400 cm^{-1}. Analytical TLC was performed on pre-coated silica gel plates (SiO_2, Merck PF_{254}). Absorption spectral investigation of **C4SB** and its complexes were performed on a Perkin Elmer Lambda-35 double beam spectrophotometer using standard 1.00 cm quartz cells, whereas emission spectra were recorded on a Photon Technologies International Quanta Master Spectrofluorimeter (model QM-4/2006).

Synthesis

Synthesis of target compound (**4**), *i.e.*, **C4SB** was carried out by stepwise synthesis as shown in Scheme 1. The starting material *p-tert*-butylcalix[4]arene (**1**), dinitro derivative of *p-tert*-butylcalix [4]arene (**2**) and its aminated derivative (**3**) were prepared by earlier published procedures.[50,51]

Synthesis of C4SB

0.5 g (0.58 mmol) of compound **3** was dissolved in 10 ml absolute ethanol and 0.3 g (1.16 mmol) of 2-hydroxynaphthaldehyde was added to the reaction mixture with stirring for 30 min followed by refluxing (36 h). The mixture was cooled and poured in cold water to obtain a light greenish yellow precipitate. The precipitate was filtered and washed with ethanol and dried for further crystallization from dichloromethane/methanol to furnish compound **4**. Yield (0.6 g, 0.51 mmol, 68%); m.p. 285 °C decompose, FT-IR (KBr): 3353 cm^{-1} (˙OH), 1651 cm^{-1} (C═O), 1601 cm^{-1}, 1480, 1361 and 1232 cm^{-1} (N–H), 1190 cm^{-1} (C–N); ^{1}HNMR (400 MHz, DMSO, TMS, ppm): δ_H: 1.11 (18H, s, *t*-Bu), 1.17 (18H, s, *t*-Bu), 2.48 (4H, s, $ArCH_2$–O) 3.47 (4H, d, J = 13.2 Hz, Ar*CH*$_2$Ar), 4.1 (4H, d, J = 13.2 Hz, Ar*CH*$_2$Ar), 5.1 (2H, s, Ar *Napth* –*OH*), 6.73 (4H, s, Ar*H*), 6.84 (4H, s, Ar*H*), 7.1 (8H, s, Ar *Benz*), 7.18 (2H, s, Ar –*OH*),7.30 (4H, trip, Ar *Napth*), 7.5 (2H, s, Ar *Napth*), 7.6 (2H, d, Ar *Napth*), 8.0 (2H, d, Ar *Napth*), 8.2 (2H, s, N═C–H) (Fig. S1 ESI†), δ_C: 31.4, 31.5, 32.9, 34.1, 75.8, 118.4, 123.3, 123.7, 124.1, 125.2, 126.6, 126.8, 128.0, 128.4, 132.1, 158.5, 160.3, Anal. calc. for $C_{80}H_{80}N_2O_6$; C, 82.47; H, 8.47; N, 2.40 found: C, 82.96; H, 8.25; N, 2.36.

Synthesis of metal complexes

Saturated solutions of **C4SB** in THF were prepared in round bottomed flasks. Stoichiometric amounts of Al^{3+} and I^- were added into each respective flask. The mixture was stirred at room temperature for 24 hours. The solution was filtered and the remaining residue was washed with small amounts of water. The filtrate was evaporated at reduced pressure. The resultant crystals were dried in a vacuum oven.

Spectroscopic measurements

UV-visible and fluorescence studies of **C4SB** with different metals and anions were performed at a specific concentration of both host and guest. A stock solution of ligand (2.6×10^{-3} M) was prepared in 25 ml of THF followed by dilution (2.58×10^{-5} M) to 100 ml. Fluorogenic behavior of receptor **C4SB** was investigated using titration experiments in a binary solvent composition of THF : H_2O (1 : 1 v/v). Ten molar eq. of each metal and anion were measured using a 1 cm absorption cell. In 10 ml test tubes, 2 ml of ligand solution of (2.6×10^{-5} M) and 2 ml of metal/anion salts solution (2.6×10^{-4} M) were mixed together. The UV-visible response of the ligand before and after addition of the ion solution was recorded. Emission intensities of **C4SB** were measured at 330 nm for metals and 280 nm for anions at room temperature. For the interference study of coexisting ions, 10 equivalent solutions of other metals (2.6 ×

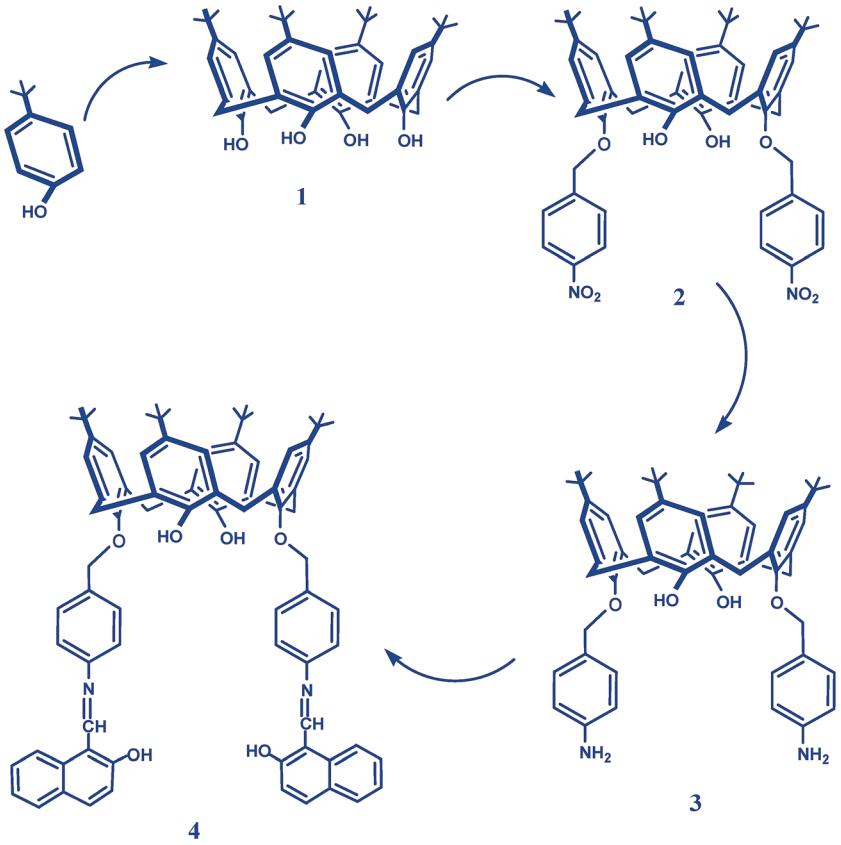

Scheme 1 Synthesis of resin **C4SB**: (1) $HCHO/OH^-$, (2) $BrCH_2C_6H_4NO_2/K_2CO_3$, (3) $NH_2NH_2 \cdot H_2O$/RANEY® Ni, (4) 2-hydroxynapthaldehyde.

10^{-4} M) were taken into the same solvent system containing **C4SB** complexes with Al^{3+}/I^-.

Determination of complex stoichiometry

The continuous variation method, *i.e.*, Job's plot,[52] was applied for the determination of stoichiometric ratios of **C4SB** with Al^{3+} and I^- in THF and H_2O as a binary solvent system. For this method equimolar solutions (2.6×10^{-5} M) of both host and guest, *i.e.*, **C4SB** and Al^{3+}/I^-, were mixed under the conditions where the ligand–metal concentration remained constant. The absorbance was measured at 230 and 220 nm for Al^{3+} and I^- complexes, respectively.

Results and discussion

UV-visible study

To examine the chromogenic behavior and selectivity of **C4SB** titration experiments were carried out in THF : H_2O binary solvent system for a selected series of mono, di and tri valent cations: Li^+, Na^+, K^+, Rb^+, Cs^+, Ag^+, Ba^{2+}, Ca^{2+}, Mn^{2+}, Mg^{2+}, Sr^{2+}, Ni^{2+}, Cd^{2+}, Co^{2+}, Cu^{2+}, Hg^{2+}, Pb^{2+}, Zn^{2+}, Fe^{2+}, Fe^{3+} and Al^{3+}. Preliminary investigations reveal that the **C4SB** ligand before complexation exhibits two characteristics bands. One band at 280 nm is comparatively smaller in absorption than the other band at 220 nm. These absorption bands are ascribed to the π–π* and n–π* transitions, respectively (Fig. 1). There were nominal changes occurring and only a minimal enhancement in the absorption intensities observed upon contact with different metal ions. However, on addition of Al^{3+} a prominent change is noticed in the absorption behavior of **C4SB**. A hyperchromic shift along with a bathochromic shift was observed from 220 nm to 230 nm, and the band intensities were surprisingly enhanced from 0.8 to 1.6 (Fig. 1). This spectral change upon formation of the **C4SB**–Al^{3+} complex at 221 and 280 nm could be due to the π-electrons of the (C=N) imine aromatic rings and the lone pair of electrons present on the oxygen/nitrogen atoms altering to O/N-metal charge transfer absorption upon Al^{3+} contact.[53]

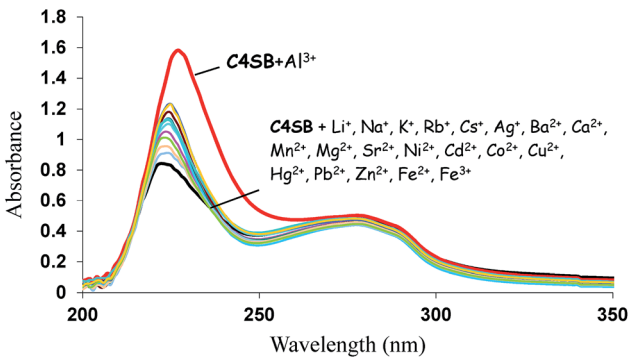

Fig. 1 Absorption spectra of **C4SB** (2.6×10^{-5} M) and with different metals (10 eq.) in THF and H_2O.

The selectivity and binding ability of **C4SB** for different anions like F^-, Cl^-, Br^-, I^-, CO_3^{2-}, HCO_3^-, $CH_3CO_2^-$, SO_4^{2-}, HSO_4^-, CN^-, SCN^-, NO_3^-, ClO_4^-, $Cr_2O_7^{2-}$ and S_2O_7 were also investigated under the same conditions (Fig. 2). The distinctive UV-visible absorption changes were recorded upon addition of a sodium salts solution of the anions to **C4SB** (2.6×10^{-5} M). Different anions produced slight variations in spectral properties of **C4SB**. However, there was a dramatic effect observed in the spectral response of **C4SB** on addition of I^- which caused the emergence of two new bands at 366 nm in the visible region. While a hyperchromic effect along with red shift was observed in the bands at 280 and 220 nm. These bands at 280 and 220 nm shifted ≈14 and 12 nm to a longer wavelength region, respectively. Strong absorption in the region of 220 nm along with the appearance of a new band in the visible region at 335–430 nm is the indication of complex formation. **C4SB**–I^- selective complexation can be explained by the hydrogen bond interaction between I^- and the hydroxyl protons (–OH) of **C4SB**. This response suggests very strong and selective affinity of **C4SB** towards Al^{3+} and I^-. The presence of a hard donor site for hard acid and the involvement of hydrogen bonding reflects the dual selectivity. Besides this thermodynamic stability, ionic radii, cavity size as well as geometry of the ligand and ions are also important aspects for specificity which add to the affinity of the ligand towards both the cation and anion.

Fluorescence study

Further exploration into the fluorescent behavior of **C4SB** with different metal ions was performed under the same conditions as the UV-visible studies. The titration measurements were carried out with 10 eq. of ions and 2.6×10^{-5} M **C4SB**. The fluorescence response of **C4SB** did not produce any substantial variations upon interaction with the metals, however, it did exhibit a prominent fluorescence response toward Al^{3+}. Addition of a small amount (10 eq.) of Al^{3+} into the solution of **C4SB** (2.6×10^{-5} M) causes the formation of a new stronger band with high emission intensity at 398 nm. The emission intensity at band 398 nm was increased up to 95 fold (Fig. 3). This result obtained after Al^{3+} addition confirms that **C4SB** has potential as a selective Al^{3+} probe. The increase in fluorescence during complexation is attributed to deactivation of the PET

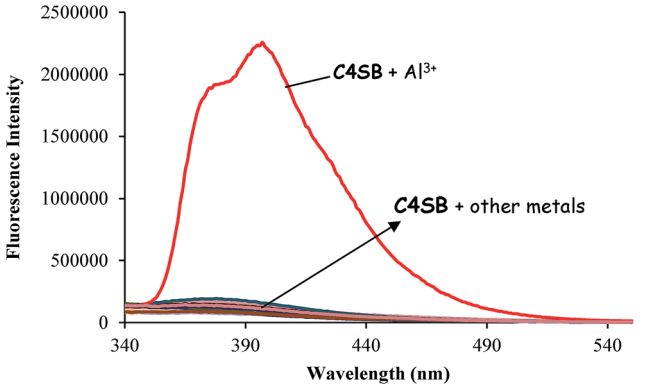

Fig. 3 Fluorescence emission spectra of C4SB (2.6×10^{-5} M) and C4SB with different metals (10 eq.) in THF and H_2O at 330 nm.

(photoinduced electron transfer) process occurring between the 2-hydroxy naphthalene moiety and the imine functional group site. Upon contact within the **C4SB** cavity, the electrons of O and N drift to Al^{3+} and thus diminish the PET process by reducing the delocalization into the naphthalene ring.[54]

Similarly more investigations were also carried out for **C4SB** as an I^- selective fluorogenic sensor. The selective response of **C4SB** for I^- was reflected by the prominent fluorescent changes after interaction with I^- anions. The strong emission band at 309 nm in the parent spectrum was dramatically quenched upon addition of (10 eq.) of I^-. The considerable 85% reduction in the emission intensity was ascribed to the formation of the **C4SB**–I^- complex (Fig. 4). No substantial fluorescence variations were observed in the presence of (10 eq.) of other anions, which confers the high specificity of **C4SB** toward I^-. Furthermore, the change in fluorescence intensity of both ions was measured by repeating the process four times. The fluorescent response of both complexes with error bars are shown in Fig. S2(a) and (b), ESI†.

C4SB exhibits a very low fluorescence intensity at 398 nm due to the PET mechanism, as **C4SB** contains 2-hydroxy naphthalene and phenyl fluorophore rings along with an imine functional group having N and O electron donating atoms. Two hydroxyls are blocked by intramolecular hydrogen bonding

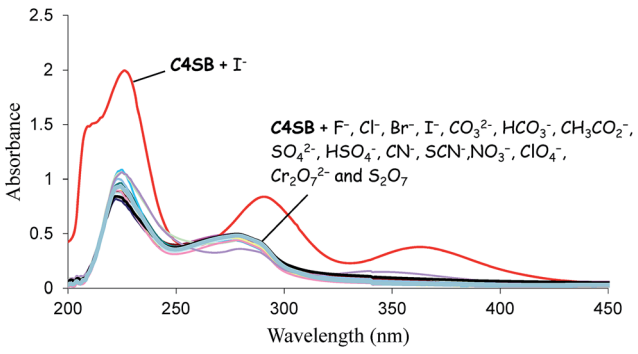

Fig. 2 Absorption spectra of C4SB (2.6×10^{-5} M) and C4SB with different anions (10 eq.) in THF and H_2O.

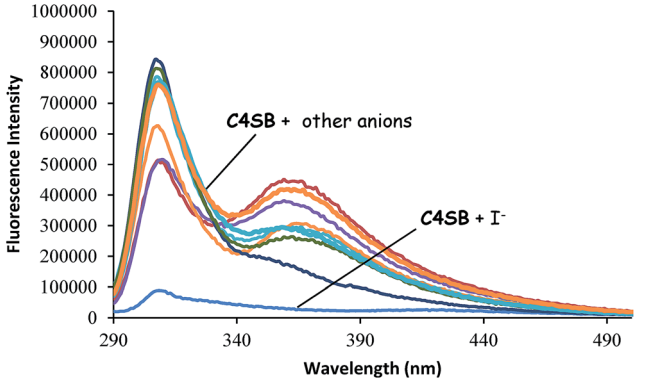

Fig. 4 Fluorescence emission spectra of C4SB (2.6×10^{-5} M) and C4SB with different anions (10 eq.) in THF and H_2O at 280 nm.

while the N atom in the imine group conjugates its electrons with fluorophore rings that switch on the PET process causing complete quenching of the fluorescence response of the probe. After bonding with Al^{3+}, the remarkable fluorescence enhancement is mainly induced by the Al^{3+} residing within the macrocyclic cavity of **C4SB** and coordinating with the N and O donors. The intramolecular PET fluorescence quenching effect derived from the electron pairs of N and O donor atoms to the fluorophores are subsequently fully blocked and relieved as the electronic density of the lone pairs is relieved through metal–donor binding interactions, consequently increasing the **C4SB** emission.

On the other hand the large quenching of fluorescence emission upon contact with I^- is the distinguishing feature among the other anions. This quenching behavior is attributed to the formation of hydrogen bonding between I^- and hydroxyl protons of the fluorophore rings. This hydrogen bonding increases the electron density on the hydroxyl oxygen atom which conjugates its electron pairs in the fluorophore ring. Thus, the PET process is triggered where the lone pair of electrons from N and O donate to the fluorophore and result in the fluorescence being quenched upon interaction with I^-.

Thus, the large quenching of emission in the presence of I^- is the characteristic feature of **C4SB** for the fluorometric identification of I^-. Other ions may also be responsible for some quenching of emission but have a relatively small effect as their size and characteristics within the **C4SB** cavity binding site are not as compatible as for I^-.

Concentration effect

Quantitative binding of **C4SB** for Al^{3+} and I^- was evaluated by examining the fluorogenic behavior when gradually increasing their concentration. There were spectral variations noticed with addition of up to 10 eq. Linear enhancement in the fluorescence intensity at 445 nm was observed with the increase of Al^{3+} ion concentration (Fig. 5 inset). The binding of Al^{3+} to **C4SB** reduced the electron-donating ability of N and O to the aromatic rings, thus suppressing the PET process and causing a remarkable increment in the emission intensity as shown in (Scheme 2). Therefore **C4SB** displays a clear 'turn-on' fluorescence response and has considerably high selectivity towards Al^{3+}. While upon addition of I^-, **C4SB** emission intensity was quenched slowly with increasing concentration (Fig. 6). Gradual increases in concentration strengthen the hydrogen bonding of I^- which in turn reinforces the electron density to fluorophore that enhances the PET process causing significant quenching of emission as shown in (Scheme 2). By plotting the ratiometric variations in the fluorescence intensities as a function of Al^{3+} and I^- ion concentrations, a Hoerl curve was obtained and is shown in the inset of (Fig. 5b and 6b).

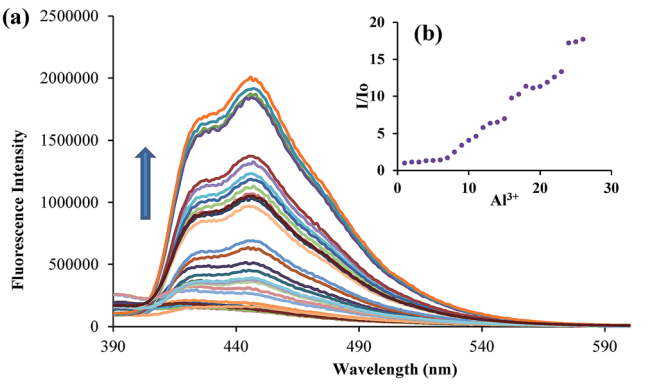

Fig. 5 Influence of the addition of increasing amounts (0 → 10 eq.) of Al^{3+} on the emission spectra of **C4SB** (2.6×10^{-5} M) in THF and H_2O.

Complexation binding constants of **C4SB**–Al^{3+}/I^- complexes were also determined by using the Benesi–Hildebrand equation.[55] A plot of the ratio $I_0/(I - I_0)$ against $[1/[Al^{3+}/I^-]$ as in the value of log K was calculated as 2.49×10^5 ($R^2 = 0.99$) for **C4SB**–Al^{3+}, and 9.24×10^3 for **C4SB**–I^- ($R^2 = 0.98$).

Job's plot

The binding extent of **C4SB** was estimated by determining the stoichiometric ratio of the complexes. Therefore Job's plot was used to evaluate the stoichiometry of **C4SB**–Al^{3+} and **C4SB**–I^- complexes at 221 nm. The results are depicted in Fig. S3(a) and (b) ESI†. The plot of absorbance against mole fractions indicates that maximum absorption values for both complexes touches 0.5, which infers that **C4SB** coordinates 1 : 1 with Al^{3+} and I^-. Furthermore, the complexes were analyzed using ESI-MS (Fig. S6 and S7†). The peak at 1163 m/z corresponds with **C4SB** $[1 + H]^+$. While peaks at 1540 and 1335 m/z correspond to **C4SB**–Al^{3+} and **C4SB**–I^- complexes, respectively.

Interference study

Functional properties and the selective nature of **C4SB** towards Al^{3+} was investigated in the presence of coexisting metal ions. Competitive experiments were carried out by using 10 eq. of other metal ions. No significant spectral variations were noticed in absorption behavior. Similarly the efficiency and potential application of **C4SB** for I^- was also examined and there was no prominent change observed in the presence of other anions. Furthermore, interfering behavior for both metal and anions was envisioned by the change in ratiometric absorption behavior (A/A_0) by the incorporation of other guest ions as shown in Fig. S4 and S5 ESI†. Representative ratiometric absorption change (A/A_0) clarifies that only Hg^{2+} shows a remarkable change among the metal ions used for testing the Al^{3+} selectivity. Due to Hg^{2+} interference the (A/A_0) value of **C4SB**–Al^{3+} complex decreased slightly from 1 to 0.97 as shown in Fig. S4†.

Various parameters like the compatible nature of binding sites for guest, ionic radii, electronegativity as well as HSAB theory are responsible for the selective complexation property of **C4SB** for Al^{3+} and I^-. Moreover, **C4SB** possesses a hard coordination site having N, O and C=N binding groups which implies a selective response to hard acid Al^{3+} which traditionally follows Pearson's HSAB theory.[53] **C4SB** is actually a Schiff base with nitrogen and oxygen-rich coordination environments for detection of hard-acid Al^{3+}, and this complements reports in literature of some Al^{3+} selective Schiff bases possessing similar

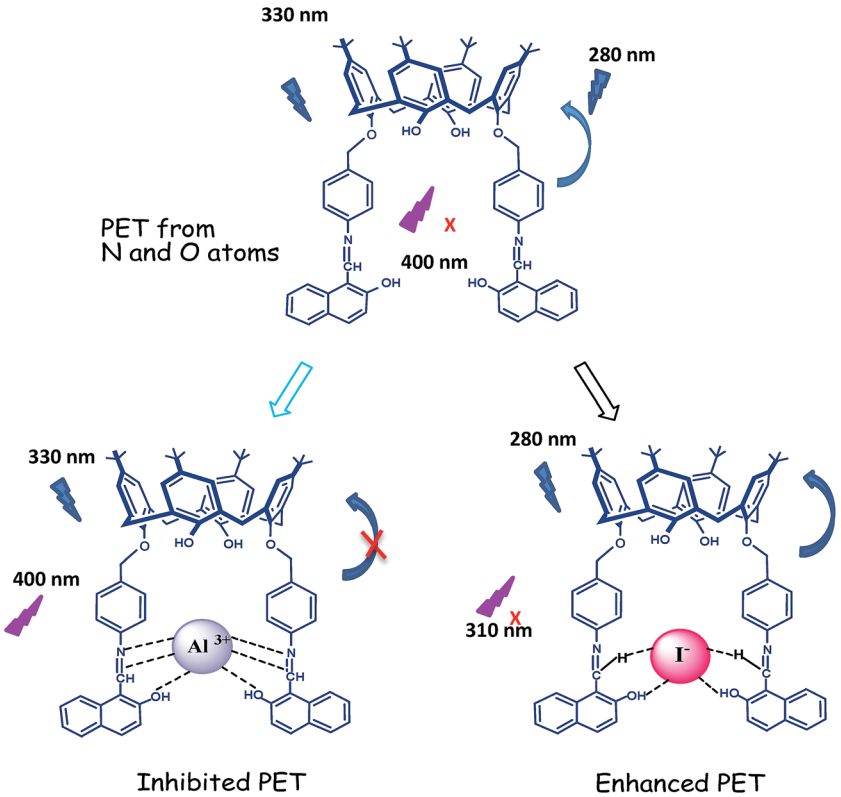

Scheme 2 Fluorescence mechanism of **C4SB** toward Al^{3+} and I^-.

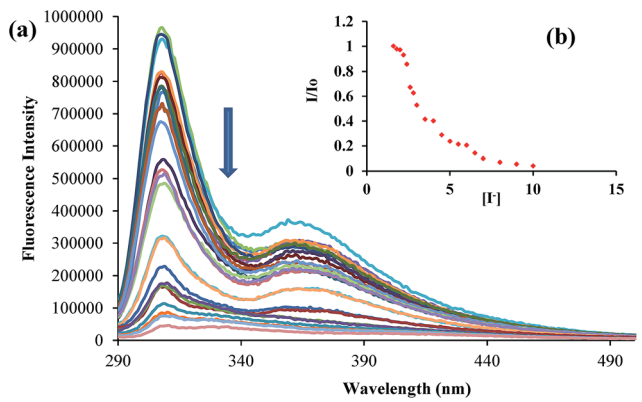

Fig. 6 Influence of the addition of increasing amounts (0 → 10 eq.) of I^- on the emission spectra of **C4SB** (2.6×10^{-5} M) in THF and H_2O.

binding sites.[56–61] This coordination is due to the presence of the lone pairs of electrons on nitrogen, oxygen and π electrons of imine (–C=N–) in the periphery of calix[4]arene moiety which favors the interaction with low polarizable hard acid Al^{3+}, and the conformity of ionic radii of metals with the cavity size of calixarene framework. A slight disturbance in the selective behavior for Al^{3+} by Hg^{2+} is due to the binding sites as well as ionic cavity conformity. Beside this, the presence of hydroxyl protons of naphthalene aromatic rings are accessible for hydrogen bonding with I^- as well. Which reflects the selective nature of **C4SB** for I^-.

FT-IR study

Since FT-IR spectroscopy helps to understand the functionalities and changes in structure after complexation, the selective response of **C4SB** toward Al^{3+} and I^- was further characterized. Free **C4SB** shows its various characteristic peaks as shown in (Fig. 7a). A broad but less intensive band from 3600–3400 cm^{-1} is due to the ν(O–H) group stretching and small broad, sharp and weak bands from 3100–2800 cm^{-1} are due to the symmetric and antisymmetric ν(C–H) stretching modes of the aliphatic as well as aromatic methyl and methylene groups. Additionally, bands at 1635 cm^{-1} indicate the ν(C=N) azide functional group, 1607 cm^{-1} ν(C=C) aromatic rings, 1518 cm^{-1} ν(H–N=C), 1481 cm^{-1} ν(C=C), 1457 cm^{-1} ν(C–O–H), 1361 cm^{-1} ν(O–H)

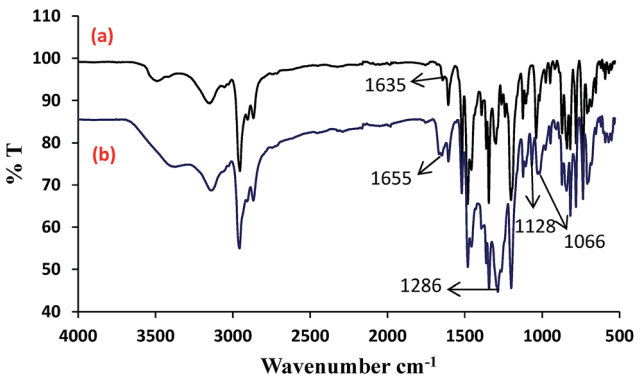

Fig. 7 FT-IR spectra (a) **C4SB** and, (b) **C4SB**–Al^{3+} complex.

bending, 1345 cm^{-1} and 1299 cm^{-1} for ν(C–N), 1262 cm^{-1} and 1239 cm^{-1} (C–O), 1201 cm^{-1} (C–N), 1124 cm^{-1}, 1108 cm^{-1} and 1038 cm^{-1} ν(C–O–C) of calix[4]arene rings. After complexation, the spectrum of **C4SB** shows distinctive variations in terms of shifting, disappearance and appearance of new bands (Fig. 7b). On complexation with Al^{3+} the band at 1635 cm^{-1} shifted to 1655 cm^{-1}. Besides this, the bands at 1391, 1299, 1262, 1240 and 1038 cm^{-1} disappeared and a new band at 1286 cm^{-1}, 1128 and 1066 cm^{-1} appeared in the spectrum of **C4SB**–Al^{3+} complex. These changes are due to metal–nitrogen/oxygen stretching and bending vibrations giving clear indication of the involvement of nitrogen and oxygen donor atoms with Al^{3+}.

In the case of I^- complexation some evidence shows the strong interaction of **C4SB** with the I^- (Fig. 8b). The band at 3492 cm^{-1} corresponds to the hydroxyl protons upon complexation and the intensity of this band increased along with a blue shift to 3423 cm^{-1}. This was due to the hydroxyl protons engaging in hydrogen bonding with I^-. The bands at 1635 and 1607 cm^{-1} merged together and appeared as a strong single band at 1620 cm^{-1}. Another band at 1518 cm^{-1} decreased upon complexation. The intensity of the band at 1345 cm^{-1} decreased. Moreover, the band at 1042 cm^{-1} completely disappeared and new bands appeared at 1550, 1104 and 1066 cm^{-1}. This indicates hydrogen bonding with I^- changed the electronic cloud on the hydroxyl oxygen. These spectral changes support the formation of the **C4SB**–I^- complex.

The selective chromogenic response of **C4SB** for Al^{3+} and I^- is strongly evidenced by the shifting, disappearance and appearance of various specific functional group bands when a guest is introduced into the receptor cavity.

Conclusions

The fluoroionophoric behavior of 2-hydroxynaphthalimine functionalized calix[4]arene Schiff base, **C4SB**, towards a series of selected different metals and anions was explored. **C4SB** displayed excellent selectivity for Al^{3+} as a turn-on sensor over a broad range of tested metal ions with remarkably enhanced fluorescent intensity. It also exhibited high sensitivity toward I^- with a turn-off fluorescence response. The Experimental results clarify the selective sensing ability of **C4SB** toward Al^{3+} and I^- even in the presence of other competing ions. Only Hg^{2+} interferes in Al^{3+} detection. The stoichiometric ratio indicates that **C4SB** forms 1 : 1 complexes with both Al^{3+} and I^-. Moreover, the formed complexes were characterized and confirmed using FT-IR spectroscopy. The geometry and ideal binding site of **C4SB** contains N, O and possesses compatible size and characteristics for both Al^{3+} and I^-. Furthermore, the selective response of **C4SB** for guests helps supramolecular systems detect and determine these toxic ions in aqueous media.

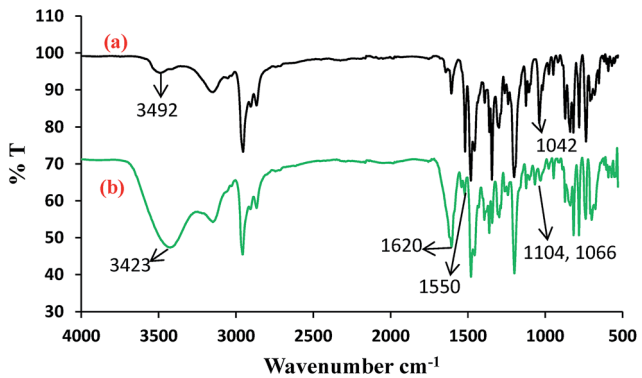

Fig. 8 FT-IR spectra (a) **C4SB** and, (b) **C4SB**–I^- complex.

Acknowledgements

We thank the National Center of Excellence in Analytical Chemistry, the University of Sindh, Jamshoro/Pakistan and the Scientific and Technological Research Council of Turkey (TUBITAK, B.02.1.TBT.0.06.01-216.01/895–6391) for the financial support of this work.

References

1 G. H. Robinson, *Chem. Eng. News*, 2003, **81**, 54.
2 D. Das, M. Dutta and S. Das, *Anal. Methods*, 2013, **5**, 6262.
3 A. Jeanson and V. Bereau, *Inorg. Chem. Commun.*, 2006, **9**, 13.
4 R. J. P. Williams, *Coord. Chem. Rev.*, 2002, **228**, 93.
5 R. O. Brown, L. M. Morgan, S. K. Bhattacharya, P. L. Johnson, G. Minard and R. N. Dickerson, *Ann. Pharmacother.*, 2008, **42**, 1410.
6 J. J. Spinelli, P. A. Demers, N. D. Le, M. D. Friesen, M. F. R. Lorenzi and R. P. Fang, *Cancer. Causes Control*, 2006, **17**, 939.
7 G. C. Woodson, *Bone*, 1998, **22**, 695.
8 B. Wang, W. Xing, Y. Zhao and X. Deng, *Environ. Toxicol. Pharmacol.*, 2010, **29**, 308.
9 V. K. Gupta, A. K. Jain and G. Maheshwari, *Talanta*, 2007, **72**, 1469.
10 P. D. J. Darbre, *Inorg. Biochem.*, 2005, **99**, 1912.
11 C. Exley, L. Swarbrick, R. K. Gherardi and F. J. Authier, *Med. Hypotheses*, 2009, **72**, 135.
12 J. Barcelo and C. Poschenrieder, *Environ. Exp. Bot.*, 2002, **48**, 75.
13 B. Valeur and I. Leray, *Coord. Chem. Rev.*, 2000, **205**, 3.
14 R. Martinez-Manez and F. Sancenon, *Chem. Rev.*, 2003, **103**, 4419.
15 S. Nabavi and N. Alizadeh, *Sens. Actuators, B*, 2014, **200**, 76.
16 G. H. Michael and S. G. Robert, *Modern Nutrition in Health and Disease*, Lea and Febiger, Philadelphia, PA, USA, 4th edn, 1968.
17 G. Dai, O. Levy and N. Carrasco, *Nature*, 1996, **379**, 458.
18 E. N. Pearce, *Arch. Intern. Med.*, 2012, **172**, 159.
19 S. E. Matthews and P. D. Beer, in *Calixarenes*, ed. Z. Asfari, V. Böhmer, J. Harrowfield and J. Vicens, Kluwer Academic, Dordrecht, 2001, ch. 23.
20 X. R. Xu, H. B. Li, J. D. Gu and K. J. Paeng, *Chromatographia*, 2004, **60**, 721.
21 Z. Huang, K. Ito, A. R. Timerbaev and T. Hirokawa, *Anal. Bioanal. Chem.*, 2004, **378**, 1836.

22 M. C. Yebra and R. M. Cespón, *Fresenius' J. Anal. Chem.*, 2000, **367**, 24.
23 K. R. Noone, A. Jain and K. K. Verma, *J. Chromatogr. A*, 2007, **1148**, 145.
24 W. Gruber and J. Herbauts, *Analysis*, 1990, **18**, 12.
25 D. Phokharatkul, C. Karuwan, T. Lomas, D. Nacapricha, A. Wisitsoraat and A. Tuantranont, *Talanta*, 2011, **84**, 1390.
26 R. A. Agbaria, P. B. Oldham, M. McCarroll, L. B. McGrown and I. M. Warner, *Anal. Chem.*, 2002, **74**, 3952.
27 A. Ben Othman, J. W. Lee, Y. D. Huh, R. Abidi, J. S. Kim and J. Vicens, *Tetrahedron*, 2007, **63**, 10793.
28 A. Helal, H. G. Kim, M. K. Ghosh, C. H. Choi, S. H. Kim and H. S. Kim, *Tetrahedron*, 2013, **69**, 9600.
29 Q. Meng, H. Liu, S. Chenga, C. Cao and J. Ren, *Talanta*, 2012, **99**, 464.
30 L. Cao, C. Jia, Y. Huang, Q. Zhang, N. Wang, Y. Xue and D. Duc, *Tetrahedron Lett.*, 2014, **55**, 4062.
31 A. Dhara, A. Jana, S. Konar, S. K. Ghatak, S. Ray, K. Das, A. Bandyopadhyay, N. Guchhait and S. K. Kar, *Tetrahedron Lett.*, 2013, **54**, 3630.
32 H. M. Park, B. N.Oh, J. H. Kim and W. Qiong, *Tetrahedron Lett.*, 2011, **52**, 5581.
33 D. Y. Lee, N. Singh, M. J. Kim and D. O. Jang, *Org. Lett.*, 2011, **13**, 3024.
34 K. Ghosh and I. Saha, *Supramol. Chem.*, 2010, **22**, 311.
35 H. Li, C. Han and L. Zhang, *J. Mater. Chem.*, 2008, **18**, 4543.
36 H. H. Wang, L. Xue and H. Jiang, *Org. Lett.*, 2011, **13**, 3844.
37 B. Ma, F. Zeng, F. Zheng and S. Wu, *Chem.–Eur. J.*, 2011, **17**, 14844–14850.
38 D. V. Suresh, N. Ahmed, S. Youn and K. S. Kim, *Chem.–Asian J.*, 2012, **7**, 658–663.
39 H. Gómez-Machuca, C. Quiroga-Campano, C. Jullian, J. De la Fuente, H. Pessoa-Mahana, C. A. Escobar, J. A. Dobado and C. Saitz, *J. Inclusion Phenom. Macrocyclic Chem.*, 2014, **80**, 369–375.
40 J. W. Steed and J. L. Atwood, *Supramolecular Chemistry*, John Wiley and Sons, Chichester, 2000.
41 H. J. Schneider and A. Yatsimirsky, *Principles and Methods in Supramolecular Chemistry*, John Wiley and Sons, Chichester, 2000.
42 B. Verdejo, S. Blasco, E. Garcia-Espana, F. Lloret, P. Gavina, C. Soriano, S. Tatay, H. R. Jimenez, A. Domenech and J. Latorre, *J. Chem. Soc., Dalton Trans.*, 2007, 4726.
43 E. J. O'Neil and B. D. Smith, *Coord. Chem. Rev.*, 2006, **250**, 3068.
44 S. Ilhan, H. Temel, I. Yilmaz and M. Sekerci, *Polyhedron*, 2007, **26**, 2795.
45 H. M. Chawla, N. Pant, S. Kumar, N. Kumar, C. Black David St, Calixarene based materials for chemical sensors, in *Chemical Sensors Fundamentals of Sensing Materials*, ed. G. Korotcenkov, Momentum Press, New York, 2010, vol. 3, p. 300.
46 A. B. Othman, J. W. Lee, Y. D. Huh, R. Abidi, J. S. Kimd and J. Vicens, *Tetrahedron*, 2007, **63**, 10793.
47 R. Joseph, J. P. Chinta and C. P. Rao, *Inorg. Chim. Acta*, 2010, **363**, 2833.
48 J. S. Kim, S. Y. Park, S. H. Kim, P. Thuéry, R. Souane, S. E. Matthews and J. Vicens, *Bull. Korean Chem. Soc.*, 2010, **31**, 3083.
49 R. Joseph, A. Gupta, A. Ali and C. P. Rao, *Indian J. Chem.*, 2007, **46**, 1095.
50 C. D. Gutsche, M. Iqbal and D. Stewart, *J. Org. Chem.*, 1986, **51**, 742.
51 M. Tabakci, S. Memon, M. Yilmaz and D. M. Roundhill, *React. Funct. Polym.*, 2004, **58**, 27.
52 D. C. Harris, *Quantitative Chemical Analysis*, 4th edn, 1995, p. 529.
53 Z. Liang, Z. Liu and Y. Gao, *Spectrochim. Acta, Part A*, 2007, **68**, 1231.
54 A. P. de Silva, T. S. Moody and G. D. Wright, *Analyst*, 2009, **134**, 2385–2393.
55 C. F. Chow, M. H. W. Lam and W. Y Wong, *Inorg. Chem.*, 2004, **43**, 8387.
56 Y. Lu, S. Huang, Y. Liu, S. He, L. Zhao and X. Zeng, *Org. Lett.*, 2011, **13**, 5274.
57 S. Kim, J. Y. Noh, K. Y. Kim, J. H. Kim, H. K. Kang, S. W. Nam, S. H. Kim, S. Park, C. Kim and J. Kim, *Inorg. Chem.*, 2012, **51**, 3597.
58 Y. K. Jan, U. C. Nama, H. L. Kwon, I. H. Hwan and C. Kim, *Dyes Pigm.*, 2013, **99**, 6.
59 L. Peng, Z. Zhou, X. Wang, R. Wei, K. Li, Y.Xiang and A. Tong, *Anal. Chim. Acta*, 2014, **829**, 54.
60 B. K. Datta, C. Kar, A. Basu and G. Das, *Tetrahedron Lett.*, 2013, **54**, 771.
61 S. Malkondu, *Tetrahedron*, 2014, **70**, 5580.